www.vbripress.com/aml, DOI: 10.5185/amlett.2016.6147 Published online by the VBRI Press in 2016

# Thermodynamic properties of zinc oxide [001] nanowires via first principles calculations

**Venu H. Mankad[1*], Sanjeev K. Gupta[2] and Prafulla K. Jha[3*]**

[1]*Department of Physics, M. K. Bhavnagar University, Bhavnagar 364002, India*
[2]*Department of Physics, St. Xavier's College, Navrangpura, Ahmedabad 380009, India*
[3]*Department of Physics, Faculty of Science, M. S. University of Baroda, Vadodara 390002, India*

[*]Corresponding author. E-mail: venu.mankad@gmail.com (Venu Mankad ); prafullaj@yahoo.com (P.K. Jha),

**Received: 08 September 2015, Revised: 25 November 2015 and Accepted: 03 January 2016**

## ABSTRACT

The size dependent vibrational and thermodynamical properties of Zinc Oxide Nanowire (ZnO NWs) along with its bulk counterparts has been studied using the first principles calculations within density functional theory. The thermodynamical parameters such as specific heat at constant volume, entropy, internal energy and Helmholtz energy as function of temperature for the different size of nanowires are obtained and compared with the bulk ZnO in wurtzite phase. We address the effects of structural confinement on the phonon dispersion, vibrational density of states and qualitatively on the sound velocities and thermal conductance. The phonon dispersion curves for considered ZnO nanowires and its bulk counterpart indicates dynamical stability. The band gap increases from bulk to nanowire and an inverse size dependency in the case of nanowires arising due to quantum confinement. The analysis of bands character in context of growth characteristics and thermodynamical properties are also discussed. Our findings will give some reference to the insight understanding of the electronic, vibrational and thermodynamical properties of size orientation dependent ZnO nanowire. 

**Keywords:** Zinc oxide nanowires; phonon; density functional theory; specific heat; Debye temperature.

## Introduction

The novel ZnO nanostructures are expected to have great potential for sensing, catalysis, optical emission, piezoelectric transduction, and actuations [**1-3**]. The interest in zinc oxide has been renewed because its nanostructure counterparts offer unique optical, electrical and piezoelectric properties. Bulk zinc oxide (ZnO) is an ionic semiconductor that has a wide range of technological applications ranging from its use as a white pigment to use in rubber industry, where it shortens the time of vulcanization. This is mainly due to large part of number of superlative attributes of these systems, including direct band gaps, high mobility electrons and the ability to selectively dope n or p type regions. Hexagonal ZnO, a typical wide bandgap (Eg=3.37 eV) and large exciton binding energy (60 meV at room temperature) II-VI semiconductor with lattice spacing a and c =0.325 and 0.521 nm respectively has recently attracted the most intensive research for many properties and potential applications in building optical and optoelectronic nanodevices [**4-9**]. The iconicity of ZnO lies in borderline between the covalent and ionic semiconductors.

Mechanical and electromechanical properties of 1-D ZnO nanostructures have also been subject of numerous investigations because ZnO Nws form the fundamental components of nanopiezotronics [**10,11**], a new field in nanotechnology in which piezoelectric nanostructures are employed for harvesting energy in self-powered wireless nanodevices. Size dependence of Young's Modulus in ZnO Nws has been experimentally and theoretically revealed [**12**]. In particular, it has been shown that the Young's modulus of ZnO Nws with diameters smaller than about 120 nm increases dramatically with decreasing diameters. Diameter-dependent surface electronic structure also suggests strong surface effects for nanowires with diameters smaller than 40 nm [**13**].

The thermal design is an important part of the development of many nanodevices. Thermal properties like heat capacity and thermal conductivity are strongly influenced by the phonon properties particularly the vibrational density of states. This makes an important area of research to understand the laws governing the vibrational properties of nanostructured materials from high technological to fundamental point of view. Further, good knowledge of the vibrational and electronic properties of ZnO both at nanoscale and bulk level is essential to understand the transport properties and electron-phonon interaction which play an important role in device performance. In addition, the vibrational properties particularly the phonon dispersion curves are important to find the dynamically stable structure as this has been shown that the growing of other crystal phases that are unstable in bulk form is also possible. The zinc blende phase can be stabilized only by growth on cubic substrates and rock salt phase may only be obtained at relatively high pressure [**14**]. Under ambient conditions, the thermodynamically stable phase for the ZnO is that of wurtzite phase. The modification of the crystal structure during the growth of

 

nanowire can have important implications for the phonon and thermal properties of nanowires. There appears an additional optical phonon mode at the zone centre for wurtzite ZnO arising from the folding of phonon branch along Γ-L line in the zinc blende ZnO. These additional optical phonon modes result in additional phonon scattering [**15**] and reduced thermal conductivity [**16**].

Despite these advances, many ground breaking challenges remain unclear in the both understanding and controlling the size of ZnO nanowires. The electronic and optical properties of ZnO NWs are debated in the literature [**17-20**]. The density functional theory calculation of infinitely long [0001] ZnO nanowire by Xu *et al.* [**21**] indicates that the surface reconstruction plays an important role in stabilizing the nanowire. Fu-Chun *et al.* [**7**] calculated the geometrical, electronic and optical properties of hexagonal ZnO nanowires and observed a significant blueshift in comparison with its bulk counterpart. Spencer *et al.* [**22**] examined the effect of gas coverage and ethanol orientation on its adsorption on the stoichiometric and oxygen deficient nanowire surface. Liu *et al.* [**23**] investigated electrical properties of ZnO nanowires grown by vapor-phase transport growth method. The electronic properties of ZnO nanowires under a transverse electric field have been investigated by Wang *et al.* [**24**].

To our knowledge, very few systematic studies on the dimension and size dependent properties of ZnO nanowires have been made theoretically particularly using ab-initio calculations until now. Most of the ab-initio calculations have addressed structural, elastic and electronic properties [**25-30**], studies on lattice vibrational modes and vibrational density of states (VDOS) in ZnO NWs are yet to receive serious attention. The phonon dispersion relations in nanowires are expected to be significantly different from the bulk due to the confinement effects and hence this can be an important tool to probe nanowires. In addition, the phonon confinement observed in a semiconductor nanowire modifies the phonon velocities which are reflected in the phonon dispersion curves and vibrational density of states. In the present work, the first principles density functional theory (DFT) calculation of the phonon properties such as dispersion curves, VDOS and specific heat for thin ZnO NWs has been performed and compared with its bulk counterpart. The paper is organized as follows. The Computational method is presented in computational detail section followed by simulated result and discussion and finally conclusions at the end.

## Computational details

All calculations for the ZnO NWs have been performed using density functional theory with the generalized gradient approximation (GGA) using Perdew–Burke–Ernzerhof (PBE) parameterization of exchange correlation functional as implemented in the Quantum Espresso code [**31**]. These calculations are performed in super cell structures using a plane-wave basis [**32**]. The vacuum region between neighboring NWs is chosen to be about ~ 1 nm in order to avoid spurious interaction, and the plane wave energy cutoff is 40 Ry. For the Brillouin zone (BZ) integration we use a 4×4×4 and 1×1×16 sampling mesh for bulk and nanowire supercell calculations respectively. Further, we have checked convergence with cut-off energy of 50 Ry and k-point mesh of 1×1×32 by insignificant amounts: pressure by less than 0.1 GPa and electron eigenvalues by less than $10^{-4}$ Ha. The Broyde-Fletcher-Goldfarb-Shanno (BFGS) method is used for the geometry optimizations. During relaxation of the nanowires, a Gaussian broadening [**31**] with smearing parameter of 0.3 Ry is used for Brillouin zone integrations. The force on each atom is converged at 0.1 eV/Å for all optimizations. Phonon calculations are performed using density functional perturbation theory (DFPT) [**31-32**]. For the calculation of density of states (DOS), after the initial calculation='scf' Self-Consistent files task, obtaining and plotting the DOS is done by means of a non-consistent calculation (calculation='nscf'). Technically, the process requires integrating the orbital energies in the BZ1, using a special point quadrature (Blochl method, occupations='tetrahedra' [**31-32**].) together with an automatically generated uniform k-point grid (card K POINTS with option "automatic"). Specify nosym=true to avoid generation of additional k-points in low symmetry cases. They are obtained by the projecting the occupied density of states onto non-overlapping spheres using the same Gaussian-broadening The Fermi energy is displaced to zero.

The computational parameters considered in the present calculations were sufficient in leading to well converged total energy, geometrical configurations, and phonons. All constructed structures of ZnO NWs are fully relaxed before further calculations. In our case, ZnO nanowires have infinite length along the c [001] direction the axial. ZnO nanowires are placed in unit cells where the inter wire distance is larger than 5 Å, which effectively prevents the interaction with neighboring cells. It is noteworthy, since these nanostructures are often synthesized at the high temperatures, the surface passivation is not considered in our calculations. In this work, the starting point for the calculation is to optimize the bulk crystal structure for the lowest energy configuration. This is followed by the electronic structure, density of states and phonon calculations of bulk ZnO using the relaxed optimized structure. Finally, the phonon calculations are performed for nanowire configurations.

## Results and discussion

*Structure*

**Fig. 1** depicts the schematic relaxed structures of a ZnO NWs along the [001] direction with a diameter of 3.0 nm (10 atoms per unitcell of ZnO), 3.2 nm (20 atoms per unitcell of ZnO) and 5.6 nm (40 atoms per unitcell of ZnO). The initial atomic structures of ZnO NWs are constructed from the bulk wurtzite structure. In order to test the accuracy of the present ab-initio calculations to the electronic structures of the ZnO NWs, we firstly optimized the structure and calculated the self-consistent band structure along with the phonon properties of bulk wurzite ZnO crystal. We found that the optimized lattice constants as a= 3.359Å, c= 5.21 Å and u= 0.3750 Å for wurzite ZnO crystal agree well with the experimental values (a=3.249 Å, c= 5.204 Å and u=0.3819) [**33-35**]. This indicates the high accuracy of the present calculation. However, there is slight deviation from other GGA calculations [**7, 36, 37**].

 

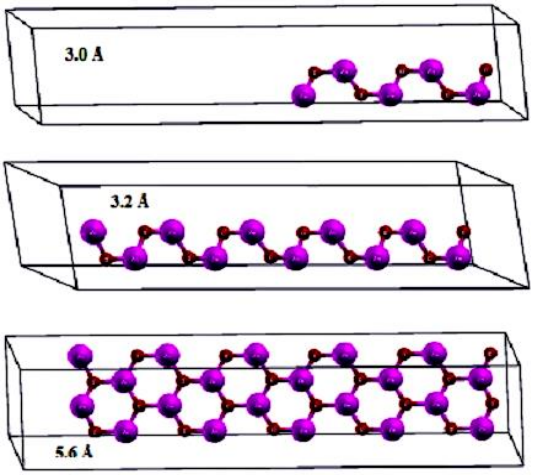


**Fig. 1**. A ball-and-stick model for different configuration of ZnO NWs along [001] direction. Relaxed structure of ZnO NWs with diameters: 3.0 Å, 3.2 Å and 5.6 Å. (Red=Oxygen and Violet= Zinc)

*Vibrational and thermodynamical properties*

The thermodynamic functions specific heat at constant volume ($C_v$), internal energy (ΔE), entropy (ΔS) and Helmholtz energy (ΔF) characterize the thermal properties of a material. To calculate these thermodynamical functions of any material the important ingredient is the phonon density of states (PhDOS) which requires the calculation of phonon dispersion curves in whole Brillouin zone (BZ) [**38-41**]. For the calculation of thermodynamical functions, quasiharmonic approximations are used [**42**]. Therefore, initially we have calculated the phonon dispersion curves and the phonon density of states. **Fig. 2**(**a**) presents the phonon dispersion curves for bulk ZnO in wurzite structure. The wurzite ZnO belongs to the space group $P_{63}mc$ or $C_{6v}$ with two formula units in the primitive cell. Each primitive cell of ZnO has four atoms. The four atoms in the hexagonal unit cell leads to twelve phonon modes, nine optical and three acoustic phonon modes. All general features of phonon dispersion curves of ZnO in wurzite structure are present and there is a good agreement with the experimental [**43-44**] and theoretical data [**45**]. However, there exist few minor discrepancies such as the longitudinal optic modes (LO) at zone centre and the splitting between the *LO* (*E*1) and the *LO* (*A*1). The phonon frequencies throughout the BZ are positive and confirm the high quality phonon calculation and dynamical stability of the considered structure.

**Fig. 2**(**b**) presents the phonon dispersion curves of ZnO NW of diameter 3.2 Å with 20 ZnO atoms in a unit cell along [001] direction of BZ. As there are 20 atoms in the unit cell there are 60 phonon branches. For clarity of the behavior of phonon branches they are enlarged and shown in the **Fig. 2**(**c-e**). Since the ZnO NWs have a lower symmetry than that of bulk ZnO, the degeneracy of many phonon modes is lifted.

In addition, quantum confinement introduces modes that do not exist in the bulk. One can observe that the vibrational modes resulting from confinement normally lies between the middle region of the acoustic and optical phonon bands with increase in the gap. The analysis of lower part i.e. acoustic phonon part of the phonon dispersion curves can be used to understand the behavior of thermal conductivity or thermal conductance of the wire as these depend on the sound velocities or slopes of the phonon branches close to zone centre of the Brillouin zone. The comparison of phonon dispersion in bulk and NW indicates lower sound velocities due to flatter acoustic phonon branches and hence the lower thermal conductivity for ZnO nanowires.

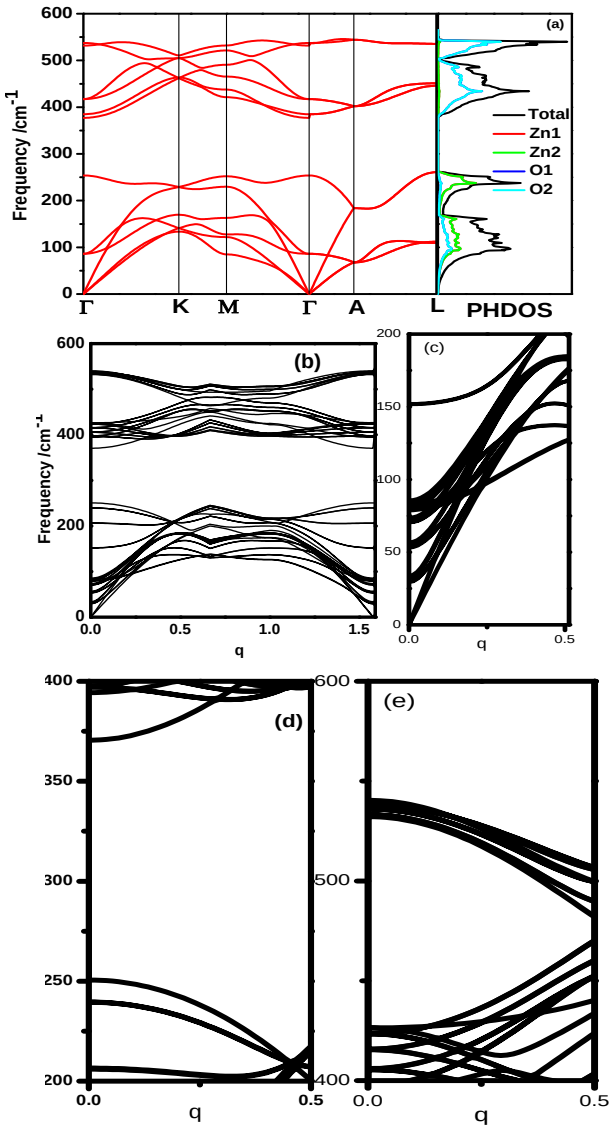


**Fig. 2**. (a**)** Phonon dispersion curves for Bulk ZnO in wurzite structure. (b) Phonon dispersion curve for ZnO NW with diameter 3.2 Å. (c) enlarged phonon dispersion curves in lower region of spectra close to zone centre (d) enlarged phonon dispersion curve in middle region of spectra close to zone centre (e) enlarged phonon dispersion curves in upper region of spectra close to zone centre.

The two lowest modes in phonon dispersion curves of NWs are flexural modes. The imaginary phonon frequencies ($w^2$(k, *j*) < 0), shown (**Fig 2**(**g**)) as negative values for the 5.6 Å diameter nanowire, represent the soft modes components define the lattice distortions and the atomic shifts, which must be performed in order to reach the stable configuration. The wave vector and the

  

irreducible representation of the soft mode which lead to lower symmetry phase, might be the candidate for a stable phase. Further, we would like to stress, that the soft modes appearing in this work (**Fig. 2(g)**), are used only as hints which tell us about the direction in which the atoms should be distorted in order to find the stable minima. This procedure considerably reduces the phase space to be searched.

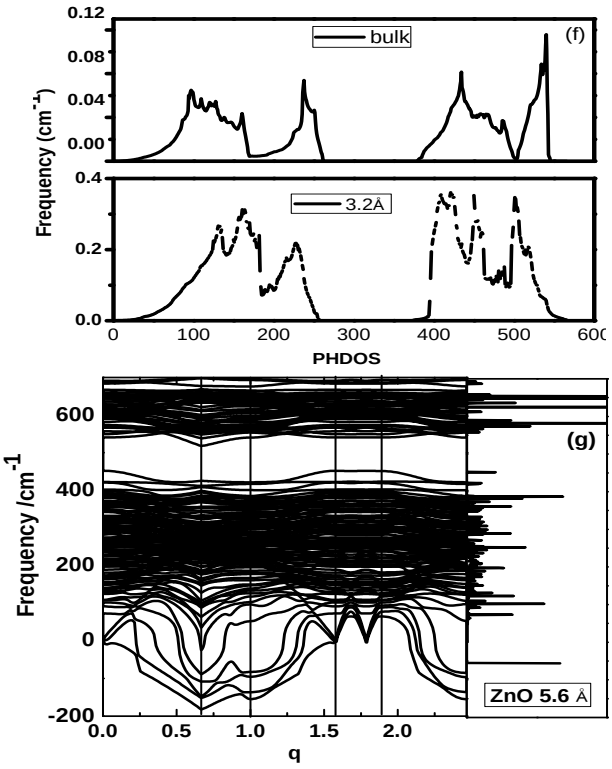


**Fig. 2.** (f) Vibrational density of state of bulk and ZnO NW with diameter 3.2 Å. (g) Phonon dispersion curve for ZnO NW with diameter 5.6 Å.

**Fig. 2(f)** presents the vibrational density of states (VDOS) of ZnO NW of 3.2 Å along with the VDOS of its bulk counterpart and depicts several obvious changes. Essentially three major features can be observed, namely the red shifting of low frequency region, weakening and broadening of several peaks and development of asymmetrical tail in the optical region of spectra. The modification of the spectra in lower frequency region can be attributed to the new features observed in acoustic phonon region of the phonon dispersion curves. We observe a clear broadening and discrimination of the peaks near 150 $cm^{-1}$. The gap between acoustic and optical region increases in the case of NW. In the high frequency region the VDOS of ZnO NW shows the distribution of peaks and increased intensity throughout the region. This can be attributed to a confinement effect of finite size effect resulting in large number of vibrational modes due to zone folding in the case of NWs [**46-47**]. Further, the VDOS is mostly related to the density of atoms in a given cross section of the NW. This being mostly the bulk property, no drastic change is observed in comparison to bulk counterpart. Therefore, we expect the thermal properties will not be the orientation dependent for nanowires.

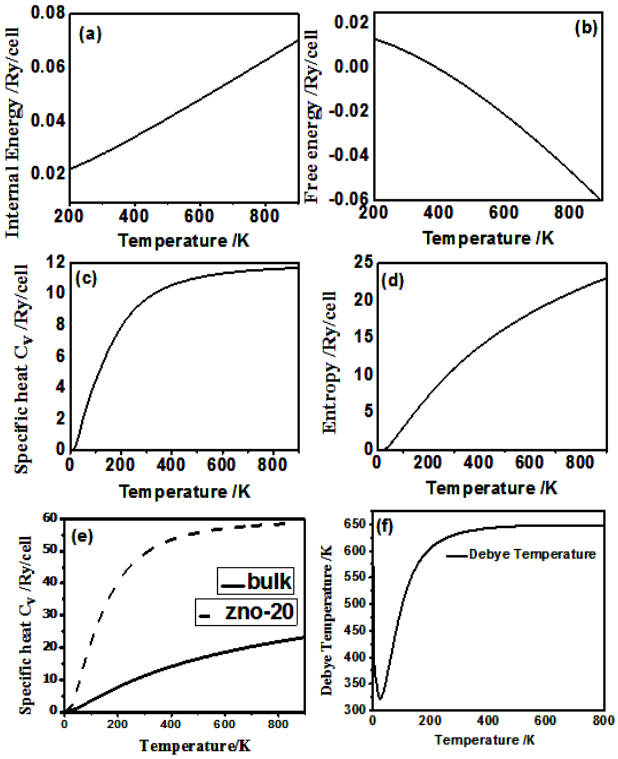


**Fig. 3.** The calculated internal energy ΔE (a), Helmholtz free energy ΔF (b), along with heat capacity at constant volume ΔCv (c), entropy S (d) bulk Lattice Specific heat as a function of temperature for ZnO bulk and ZnO NW of diameter 3.2 Å i.e ZnO-20 (e) and Debye temperature (f).

To have more comprehensive insight into the influence of phonons exerted on bulk ZnO, we have investigated the contribution of phonons to its thermodynamical properties through quasi-harmonic approximation [**45**]. **Fig. 3** presents the temperature dependent thermodynamical functions. Further we have compared lattice specific heat for ZnO bulk and ZnO NW of diameter 3.2 Å in **Fig. 3(e)**. Temperature dependent thermodynamically functions such as internal energy (ΔE), Helmholtz free energy (ΔF), heat capacity at constant volume ($C_v$) and entropy (S) presented in **Fig. 3** reveal that the internal energy (**Fig. 3(a)**) and entropy (**Fig. 3(d)**) varies linearly with temperature. However, there is a rapid change in entropy and internal energy above 100 and 200 K respectively. The heat capacity at constant volume increases above 400 K and approaches a constant value at high temperature (**Fig. 3(c)**). At intermediate temperatures, however, the temperature dependence of $C_v$ is governed by the details of vibration of the atoms and has long been determined only in experiment. The Debye specific heat theory is satisfied at low temperature. Further, the zero temperature values of internal and free energies do not vanish due to zero point motion and can be calculated from the asymptotic expression of equations given in ref [**42, 48**]. The higher frequency distribution observed in the phonon spectra is responsible for the low internal energy at low temperature as the atom has low thermal energy and hence they vibrate less, but at higher temperature the case is reverse. The successful prediction of the thermodynamical functions gives confidence in the calculation and direction to predict these properties in NWs. Our calculated thermodynamic functions for ZnO NWs are consistent with the bulk with

 

proper modification due to phonon confinement. However, we present only constant volume lattice specific heat $C_v$ for NWs. The temperature variation of constant-volume lattice-specific heat $C_v$ presented in **Fig. 3** depicts an increase of lattice specific heat with temperature until 700 K and then it gets saturated at around 55 Ry/cell (6 NK where N is Avogadro number and K is the Boltzmann's constant) the classical value as per Dulong–Petit's law. This is due to the anharmonic approximation of the Debye model. However, at higher temperatures the anharmonic effect on $C_v$ is suppressed. In comparison with the corresponding bulk ZnO, the specific heat of ZnO nanowire is lower which can be attributed to the modification of VDOS in low frequency region and blue shifting of the optical phonon modes consistent with earlier study [**47**].

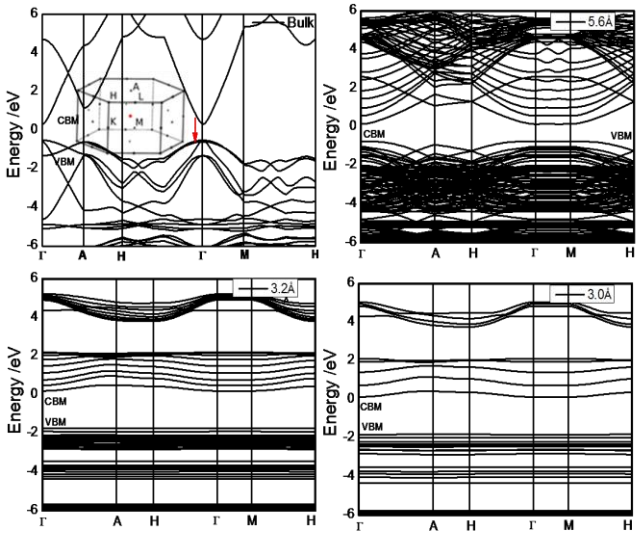


**Fig. 4.** Electronic band structures for Bulk ZnO along with other diameters 3.0 Å and 3.2 Å and 5.6 Å.

*Electronic properties*

The band structure of bulk ZnO has been calculated along lines connecting high symmetry points in the Brillouin zone (BZ) and displayed in **Fig. 4**. Our results show that both the top of the valence band and the bottom of the conduction band are located at the **Γ**- point (**k**=0), which indicates the presence of direct band gap in wurzite ZnO. The calculated bandgap is 0.87 eV, as opposed to experimental value of 3.34 eV, which is expected within the DFT calculation but is in the range of earlier calculations [**7, 36, 49**]. However, with plane wave GW calculations with the experimental lattice constants and treating the *d* electrons as core electrons relatively good agreement with experiment is achieved [**50**]. It is an established fact that the both GGA and LDA- DFT calculations always underestimated the energy gap but successful in predicting the trends. The calculated band structures along the high symmetry directions of the Brillouin zone (BZ) for ZnO-bulk and three ZnO nanowires with a diameter of 3.0, 3.2 and 5.6 Å are shown in **Fig. 4**. Clearly, the ZnO NWs retains the nature as evident from the existence of a direct semiconductor energy gap between the valence and conduction bands. The calculated band gaps of ZnO NWs are much larger than the bulk band gap. The band gap increases as diameter of the nanowire decreases. This is due to the increase in surface atoms, which have main contribution from oxygen 2p like dangling bonds [**7, 50**] and the less dispersive bands of ZnO NWs than the bands of bulk ZnO. Further, smaller the diameter of the nanowire the larger the surface to bulk atom ratio and resulting in more dangling bonds which increase the ground state energies.

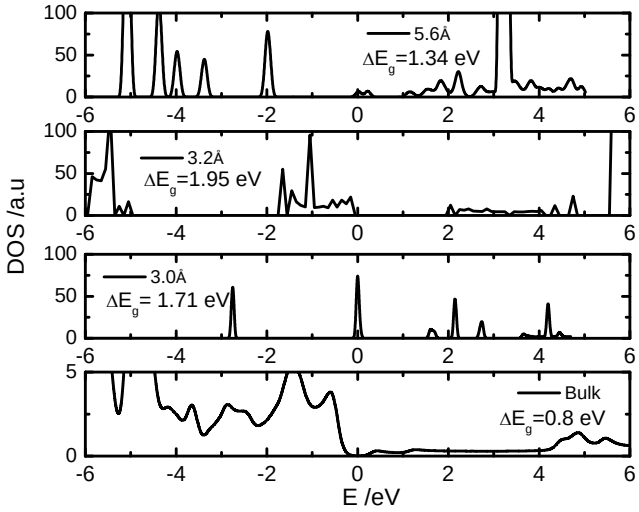


**Fig. 5.** Density of states of bulk ZnO along with the ZnO NWs with diameters 3.0, 3.2 and 5.6 Å.

We observe that the bands are dispersive in nature in VBM (range -1 to -5 eV) for nanowire of 5.6 Å which may have important implication for the better transport properties. In addition, the band-structure turns denser with the increase of diameter of NW which is due to the fact that the larger the NW, the larger is the number of electronic states. The flat bands in VBM as well as CBM along high symmetry direction (Γ-M) indicate no k-point dependency which confirms that the nanowire growth conditions in experiment are important for the application purpose. Here, we propose [001] directional growth of the nanowires for optimum use. There is 20-30 % increase of the band-gap in the smallest NWs indicating quantum confinement is very significant in nanowires. There is no Brillouin zone folding along the high symmetry directions for the bulk and NW systems, indicating weakly perturbed lowest unoccupied states arising from the confinement effect of the NW systems. There is a crossover of bands at H-point of the BZ while the bands show parabolic nature for VBM along Γ-M in nanowires, confirming the applicability of effective mass approximation.

The total electronic densities of states (DOS) of three ZnO NWs along with the bulk ZnO are presented in **Fig. 5**. An analysis of DOS together with the band structures indicates that the conduction bands originate mainly from the contribution of oxygen atoms. The valence bands above -6 eV in the case of 3.0 and 3.2 Å ZnO NWs and -4 eV in the case of 5.6 Å ZnO NWs come mainly from the Zn 3*d* orbitals. In addition, the electrons have greater mobility along the surfaces due to delocalized characters resulting from the interactions among electric charges. The *p-d* hybridizations in ZnO NWs, indicate the mixed bonding

  

semiconductor material with ionic bond much stronger than the covalent bond. The density of states, depict that the highest occupied state is mainly composed of O 2p states, while the lowest unoccupied state is mostly Zn 4*s* states. The contributions of the Zn 3d states to the top of valence bands are also seen in DOS. These are consistent with the earlier report [**7**]. These results indicate that the CBM is more sensitive to the diameter compared with the VBM. There is a remarkable change in the VBM region of DOS for the 3 Å ZnO nanowires as compared to the nanowires of other diameter mainly due to the localization of the valence band in the high symmetry regions.

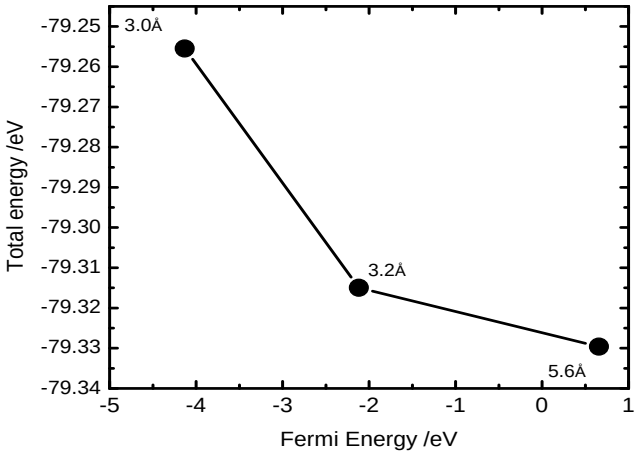


**Fig. 6.** Fermi energy Vs Total Energy curve for diameters 3.0 Å and 3.2 Å and 5.6 Å.

The analysis of change in energy gap along with the band structure and DOS reveals the importance of surface atoms and quantum confinement as the significant difference of 0.24 eV comes only from the small diameter of 0.2 Å evident from the 3.2 and 3.0 Å ZnO NWs. This can be understood from the change in total energy with respect to the Fermi energy (**Fig. 6**). **Fig. 6** shows that the variation is exponential with maximum energy for the 5.6 Å diameters. This trend is like quantum confinement effect and size variations, hence gives the confidence in the present calculations. We have connected three separate points only as a guide to eye. Our attention to show, the quantum size effect gives an exponential trend. Henceforth, we showed in terms of Fermi as it is well known that as size changes its electronic properties also change and hence Fermi level will also shift.

The high DOS near the fermi energy indicates that the structure of the nanowires is unstable (in our case 5.6 Å nanowire). We have checked this by calculating the phonon dispersion curves calculation, which indicates imaginary frequencies at Γ-point for diameter of 5.6 Å. In fact, for more stable arrangements, the states at the Fermi level almost disappear, and a true gap develops, although smaller in magnitude than the original gap of the structure [**5**].

## Conclusion

In conclusion, we have investigated the vibrational and thermodynamical properties of structurally stable ZnO nanowires. We observe a good agreement between the calculated and available phonon dispersion curves for bulk ZnO in wurtzite phase. The positive frequency of all phonon modes throughout the BZ indicates dynamical stability of the structure. There is removal of degeneracy of many phonon modes along with the appearance of several new phonon modes in the case of ZnO NW. The vibrational DOS turns to the discretization (quantum confinement) along with the significant changes in the low frequency region. In the case of ZnO NW there is a formation of asymmetric tail in the end of optical region of VDOS. The specific heat decreases in the case of nanowires. At higher temperatures the anharmonic effect on Cv is suppressed for ZnO NW. The band gap of ZnO in the present study is 0.8 eV, which is smaller than that by experiments. It is an established fact that the both GGA and LDA calculations always underestimate the energy gap. The band gap increases as the diameter of the wire decreases indicating the significance of quantum confinement. The direct band nature of bulk ZnO is retained in the case of nanowires. The bands are dispersive in the valence band maxima region suggesting for transport applications of ZnO nanowires. The density of states (DOS) revealing the potential semiconducting-like character of these nanostructures, especially if appropriate donor or acceptor atoms were available to reside in shallow states below the band edges within the bandgap. The study provides insight on how structural changes in the nanowires may affect their electronic properties, bonding character and charge transfer between atoms. This kind of study always welcome to the community of applied physics to understand the properties at base level and see how it differs from bulk material. In addition the first principles calculations are computational very costly for bigger systems. In our opinion this is not a drawback, if a conclusion can be drawn with moderate calculations.

**Acknowledgements**

This research was also supported in part by the Department of Science and Technology through computing resources provided by the High Performance Computing Facility at the Inter University Accelerator Centre, New Delhi. VM is thankful for the financial supports of the Department of Science and Technology, Govt. of India under DST Fast Track young Scientist Award grant no: SB/FTP/PS-005/2014. PKJ would like to thank DST_SERB for the financial assistance through project [SR/S2/CMP-0005/2013].

**Author Contributions**

Conceived the plan: Prafulla Jha, Venu Mankad; Performed the experiments: Venu Mankad, Sanjeev Gupta; Data analysis: Venu Mankad, Prafulla Jha, Sanjeev Gupta; Wrote the paper: Venu Mankad and Prafulla Jha. Authors have no competing financial interests.

**Reference**

1. Tian Z. R.; Voigt J.A.; Liu J.; Mckenzie B.; Mcdermott M. J.; Rodriguez M.A.; Konishi H.; Xu, H., *Nat. Mater.*, **2003**, *2*, 821
**DOI**: 10.1038/nmat1014
2. Wang Z. L. *Material Today*. **2004**, *7*, 26
**DOI**: 10.1016/S1369-7021(04)00286-X
3. Mishra Y. K.; Modi G.; Cretu V.; Postica V.; Lupan O. R.; Paulowicz I.; Hrkac V.; Benecke W.; Kienle L.; Adelung R., *ACS Appl. Mater. Interfaces*, **2015**, *7*, 14303
**DOI:** 10.1021/acsami.5b02816
4. Nomura K.; Ohta, N.; Ueda H. K.; Kamiya T.; Hirano M.; Hosono H. *Science*. **2003,** *300,* 1269.
**DOI:** 10.1126/science.1083212
5. BÄar M.; Grimm J. R.; KÄotschau A.; Lauermann Rahne I. I .K.; Sokoll S.; Lux-Steiner M .C.; Fischer C. H.; Heske C.; Jung C.; Niesen T. P.; Visbeck S. J. *J. Appl. Phys.*, **2005**, *98*, 053702.
**DOI:** 10.1063/1.2034650

 

6. Kim H. J.; Lee H. N.; Park J. C. *Curr. Appl. Phys.* **2002**, *6*, 451. **DOI:** 10.1016/S1567-1739(02)00097-4
7. Fu-Chun Z.; Zhi-Yong Z.; Wei-Hu Z.; Jun-Feng Y.; Jiang-Ni Y. *Chinese Phys. B.* **2009**, *18*, 2508. **DOI:** 10.1088/1674-1056/18/6/065
8. Kim H. K.; Kwon J. W. *Scientific Reports.***2014**, *4*, 4379. **DOI:** 10.1038/srep04379
9. Mishra Y. K.; Chakravadhanula V. S. K.; Hrkac V.; Jebril S.; Agarwal D. C.; S. Mohapatra, Avasthi D. K.; Kienle L.; Adelung R. J. *Appl. Phys.* **2012**, *112*, 064308. **DOI:** 10.1063/1.4752469
10. Wang Z.L.; Song J. *Science* **2006**, *312*, 242. **DOI:** 10.1126/science.1124005
11. Wang Z. L. *Material Today* **2007**, **10**, 20. **DOI:** 10.1016/S1369-7021(07)70076-7
12. Chen C.Q.; Shi Y.; Zhang Y.S.; Zhu J.; Yan Y. J. *Phys. Rev. Lett.* **2006**, *96*, 075505. **DOI:**10.1103/PhysRevLett.96.075505
13. Soudi A.; Dhakal P.; Gu Y. *App. Phys. Lett.* **2010**, *96*, 253115. **DOI:**10.1063/1.3456390
14. Mukhopadhyay S.; Derek S. A. *Phys. Rev. B.* **2014,** *89*, 054302. **DOI:** 10.1103/PhysRevB.89.054302
15. AlShaikhi A.;. Srivastava G. P. *Phys. Rev. B.* **2007**, *76*, 195205. **DOI:** 10.1103/PhysRevB.76.195205
16. Zhou F.; Moore A. L.; Bolinsson J.; Persson A.; Froberg L.; Pettes M. T.; Kong H.; Rabenberg L.; Caroff P.; Stewart D. A.; Mingo N.; Dick K. A.; Samuelson L.; Linke H.; Shi L. *Phys. Rev. B.* **2011**, *83*, 205416. **DOI:** 10.1103/PhysRevB.83.205416
17. Huang M. H.; Mao S.; Feick H.; Yan H. Q.; Wu Y. Y.; Kind H.; Weber E.; Russo R.; Yang P. D. *Science.* **2001**, *292*, 1897. **DOI:** 10.1126/science.1060367
18. Chen C. Q.; Shi Y.; Zhang Y. S.; Zhu J.; Yan Y. J. *Phys. Rev. Lett.* **2006**, *96*, 075505. **DOI:** 10.1103/PhysRevLett.96.075505
19. Bai X .D.; Gao P. X.; Wang Z .L.; Wang E. G. *Appl. Phys. Lett.* **2003**, *82*, 4806. **DOI:** 10.1063/1.1587878
20. Song J.; Wang X.; Riedo E.; Wang Z. L. *Nano. Lett.* **2005**, *5*, 1954. **DOI:** 10.1021/nl051334v
21. Xu H.; Rosa A. L.; Frauenheim T.; Zhang R .Q.; Lee S. T. *Appl. Phys. Lett.* **2007**, *91*, 031914. **DOI:** 10.1063/1.275714
22. Spencer M. J. S.; Wong K .W. J.; Yarovsky I. J. *Phys.:Condens. Matter.* **2012,** *24*, 305001. **DOI:** 10.1088/0953-8984/24/30/305001
23. Liu C. H.; Yiu W. C.; Au F. C. K.; Ding J. X.; Lee C. S.; Lee S. T. *Appl. Phys. Lett.* **2003,** *83*, 3168. **DOI:** 10.1063/1.1609232
24. Wang Y.; Wang B.; Zhang Q.; Shi D.; Yunoki S.; Kong F.; Xu N., *J. Appl. Phys.*, **2013,** *113*, 034301. **DOI:** 10.1063/1.4775767
25. Xiang H. J.; et al. *App. Phys. Lett.* **2006**, *89*, 223111. **DOI:** 10.1063/1.239701
26. Cicero G.; Ferreti A.; Catellani A. *Phys. Rev. B* **2009**, *80*, 201304 (R). **DOI:** 10.1103/PhysRevB.80.201304
27. Shen X.; Allen P. B.; Muckerman J. T.; Davenport J. W.; J.C. Zheng. *Nano Lett.* **2007**, *7*, 2267. **DOI:** 10.1021/nl070788k
28. Li S.; Jiang Q.; Yang G. W. *App. Phys. Lett.* **2010**, *96*, 213101. **DOI:** 10.1063/1.3435479
29. Li C.; Guo W.; Kong Y.; Gao H. *Phys. Rev. B* **2007**, *76*, 035322. **DOI:** 10.1103/PhysRevB.76.035322
30. Haffada S., Ciceroa G.; S. Madani. *Energy Procedia* **2011**, *10*, 128. **DOI:** 10.1016/j.egypro.2011.10.165
31. Baroni S.; Corso A. D.; Gironcoli S.; Giannozzi P.; http://www.pwscf.org
32. Baroni S.; Gironcoli S. de.; Corso D.; Giannozzi P. *Rev. Mod. Phys.* **2001,** *73*, 515. **DOI:** 10.1103/RevModPhys.73.515
33. Karzel H. et al. *Phys. Rev B.* **1996,** *53*, 11425. **DOI:** 10.1103/PhysRevB.53.11425
34. Kisi E.H.; Elcobe M .M. *Acta Cryst C.* **1989**, *45*, 1867. **DOI:** 10.1107/S0108270189004269
35. Decremps F.; Datchi F.; Saitta A. M.; Polian A.; Pascarelli S.; Cicco A.; DI ITIE´ J. P.; Baudelet F. *Phys Rev B.* **2003,** *68*, 104101. **DOI:** 10.1103/PhysRevB.68.104101
36. Zhang Y.; Wen Y.; Zheng J. C.; Zhu Z. *Appl. Phys. Lett.* **2009,** *94*, 113114. **DOI:** 10.1063/1.3104852
37. Erhart P.; Albe K.; Klein A. *Phys Rev. B* **2006,** *73*, 205203. **DOI:** 10.1103/PhysRevB.73.205203
38. Jha P.K.; Sanyal S. P. *Physica C.* **1996,** *261*, 359. **DOI:** 10.1016/0921-4534(96)00148-7
39. Jha P.K.; Sanyal S. P. *Phys Rev B.* **1995,** *52*, 15898. **DOI:** 10.1103/PhysRevB.52.15898
40. Jha P. K.; Sanyal S. P. *Physica B.* **1995,** *216*, 215. **DOI:** 10.1016/0921-4526(95)00438-6
41. Mankad V.; Gupta S.K.; Soni H.R.; Jha P.K. *J of Thermal Anal. and Calorimetry*. **2012,** *107*, 45. **DOI:** 10.1007/s10973-011-1576-8
42. Giannozzi P. *et al., J. Phys. Condens. Matter.*, **2009**, *21*, 395502. **DOI:** 10.1088/0953-8984/21/39/395502
43. Damen T. C.; Porto S .P. S.; Tell B., *Phys. Rev.*, **1966**, *142*, 570. **DOI:** 10.1103/PhysRev.142.570
44. Calleja J. M.; Cardona M., *Phys. Rev. B.*, **1977,** *16*, 3753. **DOI:**10.1103/PhysRevB.16.3753
45. Serrano J.; Romero A. H.; Manjo´ N. F. J.; Lauck R.; Cardona M.; Rubio A. *Phys Rev B.* **2004,** *69*, 094306. **DOI:** 10.1103/PhysRevB.69.094306
46. Gupta S. K.; JHA P K., *Solid State Commun.*, **2009,** *149*, 1989. **DOI**: 10.1016/j.ssc.2009.08.036
47. Şopu D.; Kotakoski J.; Albe K., *Phys. Rev. B.*, **2011,** *83*, 245416. **DOI:** 10.1103/PhysRevB.83.245416
48. Mankad V.; Rathod N. ; Gupta S. D.; Gupta S. K.; Jha P. K. *Mat. Phys Chem.* **2011,** *129*, 816. **DOI:** 10.1016/j.matchemphys.2011.05.014
49. Xu Y. N.; Ching W. Y. *Phys Rev B.* **1993,** *48*, 4335. **DOI:** 10.1103/PhysRevB.48.4335
50. Zakharov O.; Rubio A.; Blase X.; Cohen M. L.; G. Louie S., *Phys. Rev. B.*, **1994,** *50*, 10780. **DOI:** 10.1103/PhysRevB.50.10780


.



  